Applied Thermal Engineering 130 (2018) 477–491

Contents lists available at ScienceDirect

Applied Thermal Engineering

journal homepage: www.elsevier.com/locate/apthermeng

Research Paper

Investigation of the structure and spread rate of flames over PMMA slabs

H.R. Rakesh Ranga [a], O.P. Korobeinichev [c], A. Harish [a], Vasudevan Raghavan [a,*], A. Kumar [b], I.E. Gerasimov [c], M.B. Gonchikzhapov [c], A.G. Tereshchenko [c], S.A. Trubachev [c], A.G. Shmakov [c]

[a] Department of Mechanical Engineering, Indian Institute of Technology Madras, Chennai 600036, India
[b] Department of Aerospace Engineering, Indian Institute of Technology Madras, Chennai 600036, India
[c] Institute of Chemical Kinetics and Combustion, Novosibirsk, Russia

HIGHLIGHTS

- Experimental and numerical results of flame spread on flat PMMA slab are reported.
- Careful repeatable high resolution measurements of temperature and species fields.
- Fire Dynamics Simulator (FDS) is employed to simulate the experimental cases.
- Results from FDS have been validated against data from literature.
- Detailed structure and flow field have been presented and discussed.

ARTICLE INFO

Article history:
Received 19 September 2017
Revised 6 November 2017
Accepted 7 November 2017
Available online 8 November 2017

Keywords:
PMMA
Upward spread
Downward spread
Spread rate
Flame structure
Numerical simulations

ABSTRACT

Experimental and numerical investigations of upward and downward flame spread over flat polymethyl methacrylate (PMMA) slabs are presented here. Experiments have been carried out using PMMA slabs of different thickness in the range of 1.6 mm–5.4 mm. Downward and upward flame spread processes have been recorded under atmospheric pressure and normal gravity conditions. Careful repeatable high resolution measurements of temperature and species fields have also been carried out, to fill the scarcity of such data in literature. These data illustrate the structure and spread rates of flames established over PMMA slabs. A simple numerical model, used widely to simulate flame spread over condensed surfaces, called Fire Dynamics Simulator (FDS), has been employed to numerically simulate the experimental cases. Infinite rate chemistry and sublimation based interface model have been used. FDS is economical when compared to CFD tools such as FLUENT and OpenFOAM. It provides predictive results when compared to theoretical models. Results from FDS have been validated against numerical and experimental data from literature, by comparing quantities such as mass loss rate, flame spread velocity and flame structure. FDS is seen to capture essential transport processes of a spreading diffusion flame. Even though discrepancies have been observed between the numerical and experimental results near the fuel surface, the overall comparison of the trends has been quite reasonable. Numerical model is capable of predicting the unsteady and steady features of downward spread as well as transient rapid upward flame spread, as observed in the experimental results. Detailed structure and flow field have been presented and discussed.

1. Introduction

Requirement of detailed knowledge about the fire safety aspects has been realized in recent times, as a result of which, fire safety engineering is gaining immense importance. One of the major fire safety aspect is that of flame spreading over solid fuels and the same is dealt in this study. Knowledge about the flame spread characteristics over a condensed surface is very important to ascertain the magnitude of damage that might occur, should that material catch fire. Mostly a small flame grows to form a large fire. Hence, understanding the characteristics of small flames is an important prerequisite to understand fire spread and its growth. Flame spread leads to large fires and the process is quite complex, and is dependent on fuel type, ambient conditions and convection. On one hand, downward flame spread or flame spread over solid fuel surfaces under opposed flow condition is being extensively studied owing to its implications in fire science. On the other hand,

* Corresponding author.
E-mail address: raghavan@iitm.ac.in (V. Raghavan).

https://doi.org/10.1016/j.applthermaleng.2017.11.041
1359-4311/

upward flame spread or flame spread over solid surfaces under co-flow condition is much rapid and hazardous, and therefore, is of great interest in fire safety. Largely, investigations of fire spread process and the methods of fire prevention are usually based on detailed studies of different phenomena over the surfaces of solid materials, in general, and polymers, in particular. Although in last decade, this subject has been excessively studied by several investigators, due to its complexity, a few aspects still require additional study. One of the most actively studied polymers, which has been used in practice, is polymethyl methacrylate (PMMA). It is non-charring and has relatively simple decomposition mechanism.

Numerical and experimental studies of downward flame propagation over polymer surfaces were presented in articles by several research groups. Gong et al. [1] studied the surface and in-depth absorption effects on the thermal degradation of polymers that occurs during the process of gasification. It was reported that surface absorption leads to larger temperature gradients within the solid phase, whereas in-depth absorption leads to a fairly uniform temperature distribution within the solid phase. Consequently, for former, the controlling mechanism was found to be conduction through the solid phase and for the latter controlling mechanism was the in-depth absorption. De-polymerization of PMMA was further studied by Newborough et al. [2] using mechanically fluidized bed. Kashiwagi [3] observed various phenomena in the polymers during their burning, which had significant impact on the burning rate and flammability properties. Tewarson et al. [4] presented a detailed study of the flame characteristics such as flammability, flame spread and flame extinction, using PMMA slabs and cylinders. It was reported that the flame spread was non-accelerating for downward flame spread and accelerating for upward flame spread. The surface regression rates were reported to be very small in comparison to the flame spread rate for both upward and downward flame spread.

Mechanism of fire spread and theory of opposed flow flame spread have been vividly explained by Williams [5]. Fernandez-Pello and Hirano [6] emphasized on the controlling mechanism for the concurrent and opposed flow flame spread processes. For the prediction of concurrent flame spread rate under stable conditions, the controlling mechanism is the heat transfer from the diffusion flame to unburned fuel sample. Theoretical descriptions of flame height and heat flux, along with description of solid phase processes, were sufficient to explain the physics. Theoretical analysis based solely on the heat transfer was found to be inadequate and the effect of gas phase chemical kinetics had to be introduced at least empirically. Horizontal flame spread over polyurethane foam was studied by Tu et al. [7] under conditions of varying pressure. The smoke production in each case and the corresponding response of the smoke detector were also analyzed. It was reported that there was a significant decrease in flame spread velocity and burning rate under low pressures. Variety of experimental techniques that can be adopted in studying the laminar flame spread over solid combustibles were discussed by Fernandez-Pello and Williams [8]. Sibulkin and Lee [9] conducted flame spread rate measurements for PMMA rods of diameter in the range of 1/16 to 1/2 inches, oriented in different angles. It was also shown that cast and extruded PMMA samples burn in different manner. Temperature measurements inside burning PMMA rod and over its surface were performed with thermocouples. This data was utilized for the calculation of heat flux inside and outside of the sample. This data along with the results of other investigators were used in the subsequent work by Sibulkin et al. [10], where they obtained an analytical solution for a downward flame propagation problem for three different solid fuel geometries; finite slabs, finite rods, semi-finite fuel beds. It was found that the effect of heat transfer behind the flame and longitudinal heat conduction in the fuel become important as the fuel thickness increases.

Fernandez-Pello and Santoro [11] have conducted several experimental investigations of polymer combustion, which include downward flame spread over PMMA samples. Measurements of gas-phase velocity, and temperature in gas and solid phases were carried out in PMMA rods of different diameters. They showed that heat conduction in the solid fuel was the most important process for thermally thick samples (5 cm in diameter). For smaller rods (diameter of order of 0.16 cm) the influence of heat transfer through the gas phase was profound.

Ito and Kashiwagi [12,13] proposed holographic interferometry method for temperature measurements inside the PMMA samples near the leading edge of the flame. They carried out measurements on PMMA slabs of several widths and thicknesses, oriented under different angles. They showed that the heat transfer from the gas phase into the unburned fuel ahead of the pyrolysis location was the dominant heat transfer path for all angles of orientation, as opposed to the conductive heat transfer through the condensed phase.

Bhattacharjee et al. [14] presented flame spread rate data for PMMA slabs with varying thicknesses, burning in normal and increased (up to 50%) oxygen concentration environment at different ambient pressure conditions (from 1 atm to 0.25 atm). A comprehensive computational model was used to establish a transition criterion between the chemical and thermal regimes, and between the thin and thick fuel regimes. These results were also used in their subsequent work [15] for validation of a new simplified parabolic combustion model. In that work, comparisons of flame shape, temperature field and velocity field, between predicted and measured results were reported. Later, this model was utilized to study the flame structure in downward flame spread over thermally thin cellulose material [16]. Besides temperature measurements, Bhattacharjee et al. [16] used non-dispersive infrared radiation (NDIR) sensor to measure CO_2 concentration field in the flame. It was found that the temperature signal and CO_2 concentration, when appropriately normalized with the equilibrium values, were similar. Although, downward moving flame over thin solid fuel was often considered a laminar flame, the fluctuation data from the probes indicated that there was considerable turbulence along the outer edge of the flame.

Wu et al. [17] measured spread rate, temperature and ignition delay times for flame spread over thermally thick PMMA slabs. It was found that ignition delay time was nearly constant for the opposed flow velocities lower than 30 cm/s. Calculations of the downward spread rates with the model proposed by Wu et al. [17] were in relatively good agreement with experimental results, except in a low velocity regime. Downward flame spread over PMMA sheets of different thicknesses was experimentally studied by Ayani et al. [18], to understand the relation between the flame spread velocity and the thickness of the sample. The angle of pyrolysis and its dependence on the thickness of the sample were also reported. Downward flame spread over inclined cellulosic solids was experimentally studied by Zhang et al. [19]. Emphasis was laid on the decelerating mechanism which was analyzed using the heat and mass transfer between the solid phase pyrolysis and the gas phase combustion. A theoretical model was proposed to determine the temperature in gas- and solid phases. A numerical study of horizontal flame spread over PMMA at different forced convective velocities was reported by Ananth et al. [20]. Regression and burning rates were reported. Temperature contours and species concentration profiles at different locations were presented. Gong et al. [21] studied the influence of low ambient pressure on heat and mass transfer processes during downward flame spread over thick (3 mm–6 mm) PMMA slabs in quiescent air. At lower pressure, quenching of flames occurred below a critical Damkohler number. The same authors proposed a theoretical model to estimate the leading edge angle, mass loss rate and flame spread over

PMMA slabs of different widths (from 1.5 to 12 cm) [22]. The model also included two methods to estimate the heat flux ahead of leading edge and on the pyrolysis surface by measured mass loss rate or flame spread rate. The validity of the proposed model was verified by good agreement between the experimental and predicted results.

Consalvi et al. [23] reported detailed numerical analysis of heating up an unburned fuel sample during upward flame spread over PMMA slabs. It was reported that the continuous and intermittent flame regions have a significant role to play in the heating up of unburned sample, whereas the plume had a very little contribution to it. Upward flame spread over vertically oriented PMMA surface was experimentally and theoretically studied by Rangwala et al. [24] to determine the width effects on the flame characteristics. Diffusion of fuel vapors to the sides was significant for narrowly wide fuels and had significant effects on the flame height and spread rate. Wang and Chateil [25] have numerically studied the flame spread over horizontal surface of a condensed fuel under forced convective conditions using Fire Dynamics Simulator (FDS). They reported that the largescale flame propagation over condensed fuel surface occurred in two modes. In the first mode, flame was confined within a boundary layer and a slow increase in flame spread rate was observed. In the second mode, flame extended as a plume, and a rapid increase in flame spread rate was observed, which then reached an asymptotic value. Flame stabilization and flame extinction over aerodynamically thick non-charring fuels were numerically studied by Kumar and T'ien [26]. Two-dimensional numerical model was used for the study, in a flow configuration similar to that in the limiting oxygen index test. An opposed flow velocity was imposed on the flame during the study. It was reported that as the oxygen percentage in the opposed flow decreased, the flame, which was previously anchored to the sides of the fuel, abruptly shifts to the top surface of the fuel (wake flame). This limiting value of oxygen increased with increase in the imposed velocity. When the oxygen concentration was increased from the extinction limits, the transition from wake flame to side stabilized flame occurred at a different limit, which suggested the existence of hysteresis. Flame structure of an upward flame spreading over vertically oriented non-planar PMMA surfaces was experimentally studied by Sumit et al. [27]. Concurrent flame spread over stepped slabs were analyzed in detail. Time-dependent percentage mass lost, surface regression, OH^*, CH^* chemiluminescence, planar laser induced incandescence of soot and planar laser induced fluorescence of polyaromatic hydrocarbons (PAH) were presented. It was reported that the main effect of the step was that it caused an increase in burning rate resulting in increase in mass loss rate. The flow fields were also studied and differences in the same, between plate-ignited and step-ignited cases were reported. Insulation materials and decorative materials are widely used these days. These employ materials such as extruded polystyrene foam (XPS) which are combustible. Downward flame spread studied of these were conducted by An et al. [28]. The effect of parallel curtains and the distance between these and the insulation material were studied in detail. The average flame height was found to be higher if the distance between XPS and the curtain wall is higher. However, the average maximum flame temperature was found to increase with increase in the separation distance, but only till a particular distance. Any further increase resulted in a drop in the average maximum flame temperature. The work of An et al. [28], therefore, shows the important role played by the air entrainment during the flame spread over solid surfaces. Similar work was done by An et al. [29] where upward flame spread experiments were investigated and the results were reported.

It is clear from the literature survey that there have been several studies investigating co-flow and opposed-flow flame spread over solid fuel surfaces under different geometric and ambient conditions. Experimental data on the concentration profiles of species in a polymer flame spreading over the polymer have not been reported. These data are in great demand for developing a detailed model for flame spread over the polymer, considering the kinetics of polymer pyrolysis and the pyrolysis products, as well as the gas-phase reactions of the products combustion.

However, data on temperature and species profiles and velocity fields, in small scale samples, which can be utilized in thorough understanding of the process, are scanty. Therefore, in this study, controlled lab scale experiments using different PMMA samples have been conducted and careful measurements of mass loss rate, pyrolysis zone length, flame spread rate and species and temperature fields are reported for both upward and downward flame spread cases. FDS is a unique software that is used specially to simulate flames and fires over condensed fuel surfaces at a reasonably faster rate. Previous authors have either used the in-house CFD codes, which would take significantly longer time to simulate the flames, or theoretical models, which are simplified by several assumptions. Only a few works such as those of Wang and Chateil [25], Liang et al. [30], Hostikka and McGrattan [31], and Kwon et al. [32] have reported the use of FDS, intermediate level software, for simulating flame over condensed fuel surfaces. In this work, the capability of FDS, especially to predict gas-phase flow, species and temperature fields in heterogeneous reactive flow is demonstrated for different cases. Results from FDS have been validated against data from literature as well as that from the present experiments. For this, a simplified sublimation model for PMMA gasification is considered and appropriate grid densities to predict the mass loss rate and species and temperature profiles are used. Also, the computational cost involved in using FDS is much lesser when compared to full-fledged CFD software such as FLUENT or Open FOAM.

2. Approach

2.1. Experimental setup

2.1.1. The experimental setup for downward flame spread

The schematic of the experimental setup is shown in Fig. 1. Cast PMMA slabs (Marga Cipta brand from Indonesia) 100 mm wide and 150 mm long were inserted into a thin metal frame with low

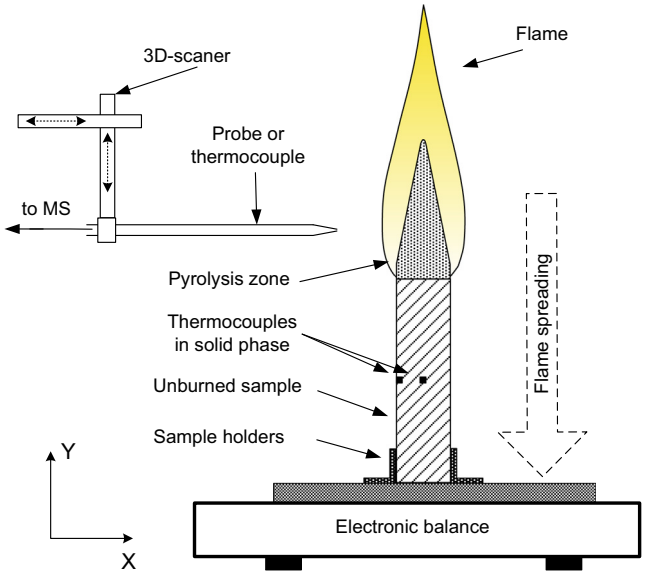

Fig. 1. The experimental setup for downward flame spread.

thermal conductivity to prevent flame spread over the side surfaces and to facilitate even flame front spreading on the center of the slab surface. The metal frame with the PMMA sample was positioned on an electronic balance for mass loss rate measurements. The flame spread velocity was derived from digital camera video recording. For this purpose, horizontal marks were made on the specimen's surface with a 10 mm step. The slabs were ignited from its top edge by the flame of a propane-butane burner. The flame had the shape of an elongated cone more than 10 cm high, allowing simultaneous ignition of the entire top edge. Flame structure measurements were performed only in the steady combustion mode, i.e., after the mass loss rate and the flame spread velocity rate became almost constant. After the experiments, the extinguished specimen was removed from the balance and cut in the middle lengthwise, in order to measure the contour of the pyrolysis zone.

To measure the temperature profiles in the fuel, type S thermocouples 50 μm in diameter were used. Thermocouples were installed in the middle of the height of the samples. One thermocouple was installed in the center of the specimen, and the other one, near its surface. The thermocouples were installed in a groove cut in the slab surface, which was glued using a 50% solution of PMMA in dichloroethane. Visual observation and flame spread velocity measurements show that there were no changes in combustion characteristics near the glued location.

The flame temperature was measured by another type S thermocouple 50 μm in diameter and coated with SiO_2 layer of 10 μm thick to prevent catalytic reactions on thermocouple surface. The diameter of its junction was 80 μm, and the thermocouple shoulders made from 50 μm wire were 5.5 mm long. The shoulders of thermocouple 4 were welded to the Pt and Pt+10%Rh wires 0.2 mm in diameter, which were placed into quartz capillaries 0.7 mm in diameter inserted into a ceramic tube 3 mm in diameter and 70 mm long. The outstanding length of the capillaries was 40 mm. Thermocouple has been fixed on a 3D-scanning device with three stepper motors, allowing the thermocouple to be moved in three coordinate directions as controlled with a computer program specially developed for the purpose. The temperature field was built based on the temperature profiles measurement data along the selected trajectories of the thermocouple's movement to the polymer surface. The design of the thermocouple allowed its contact with the slab surface without deforming its shoulders. The temperature measurement accuracy was ±50 K. The correction for radiation heat loss was assessed to be less than 100 K for the maximum temperature value. The error of the temperature measurement, related to the measurement of the emf is approximately ±30 °C. The correction for radiation heat loss for the thermocouple was estimated using the formula provided by Kaskan [33]. For the maximum measured temperature T_c = 1940 K, this correction gives 190 K.

All thermocouple signals were recorded with a 14-bit AD converter E14-140-M and synchronized with the video recording. The thermocouple's response time was ~0.05 s, and the temperature measurement rate was 1000 Hz. The chemical structure of the flame was measured using a quartz microprobe with the orifice diameter of 60 μm. The internal angle of the opening of the probe at the cone tip was 20°.

The probe was also mounted on the 3D-scanning device, and gas samples were introduced into the ion source of a Hiden HPR-60 mass-spectrometer. For all the major species discovered in the PMMA flame, such as methyl methacrylate (MMA), C_2H_4, C_3H_6, O_2, CO_2, H_2O, calibration tests were conducted, and calibration coefficients were obtained. The procedure of determining the mole fractions of the species has been described elsewhere [34]. Mole fractions were measured with an accuracy of ±10–15% for different species.

2.1.2. Experimental set up for upward flame spread

To study combustion of PMMA slabs 50 mm wide and 150 mm long, a rectangle frame 225 mm high, 85 mm wide and 22 mm deep was built, fixed on a dural base 4 mm thick. The upper part of the specimen was mounted with adhesive tape made of quartz fabric and was clamped between two stainless steel plates 1.3 mm thick. The edges of the remaining part of the specimen were exposed. The specimen clamped between the plates was placed in the slots in the upper part of the frame. The image of the burning specimen fixed inside the frame is shown in Fig. 2(a). In the right half of the frame, a window was made along the specimen 17 mm wide to allow the vertical positioning of the specimen in space to be controlled and burning of the specimen to be recorded from the side. Before the experiment, the frame with the fixed specimen was placed on an electronic balance, I-2000 with a weighing precision of 0.01 g. To ensure close contact of the frame with the balance surface, the frame base was fixed with the balance surface by plasticine balls. The lower end of the specimen was left free for ignition. The specimen was positioned strictly vertically in two mutually perpendicular directions, which was controlled with a laser level (Fig. 2b and c). The lower edge of the specimen was ignited with a gas burner. The burning process was recorded using two video cameras. One camera recorded combustion from the flat side of the specimen, as seen in Fig. 2(a), while the second one recorded combustion from the side, as seen in Fig. 2(b). The mass loss of the specimen was recorded from the electronic balance reading. Electronic digital reading was videotaped and also its data were transmitted to a computer. Fig. 2(d) shows the burnt specimen. On the sides of the frame, leads and fixtures for four thermocouples were made, located with a spacing of 20 mm. The thermocouples, originally glued into the specimen surface, can be also seen in Fig. 2(d).

In the experiment type S thermocouples have been used, welded from wire of 50 μm diameter. The thermocouples were glued into the PMMA slab in grooves, 0.2–0.3 mm deep, which have been made on the slab surface, using a 50% solution of PMMA in dichloroethane. The readings of the thermocouples were used to measure the mean flame spread rate.

2.2. Numerical model

Fire Dynamics Simulator (FDS) was used to simulate experimentally studied flames. FDS version 6.5.3 and its visualization tool, Smokeview version 6.4.4, have been used. FDS is unique software used explicitly to simulate flames and fires and is a freeware developed by National Institute of Standards and Technology (NIST), USA. The software solves numerically a form of the Navier-Stokes equations, which is appropriate for low-speed, thermal gradient induced flow [35]. An emphasis is made on smoke and heat transport from fires. This software has been validated by several researchers and is observed to predict the mass loss rate, the flame spread rate and profiles quite accurately. FDS models fluid flow using LES or DNS. In LES model of FDS, a Smagorinsky form of large eddy simulation is incorporated in the hydrodynamic model [35]. In the present study, LES sub-model in FDS has been used in laminar reactive flow simulations to study flame spread phenomenon, following the studies of Wang and Chateil [25], Liang et al. [33], Hostikka and McGrattan [31] and Kwon et al. [32]. Governing equations for mass, momentum, species and energy conservations have been solved in gas-phase [35]. In the solid phase, the energy and mass equations are solved. Buoyancy induced flow (gravity effects) were included in momentum equations. However, convective transport of liquid was not modeled.

There are several pyrolysis and gasification models available in FDS. PMMA is a non-charring type solid fuel. Table 1 shows the properties of PMMA used in the numerical model. Ananth et al.

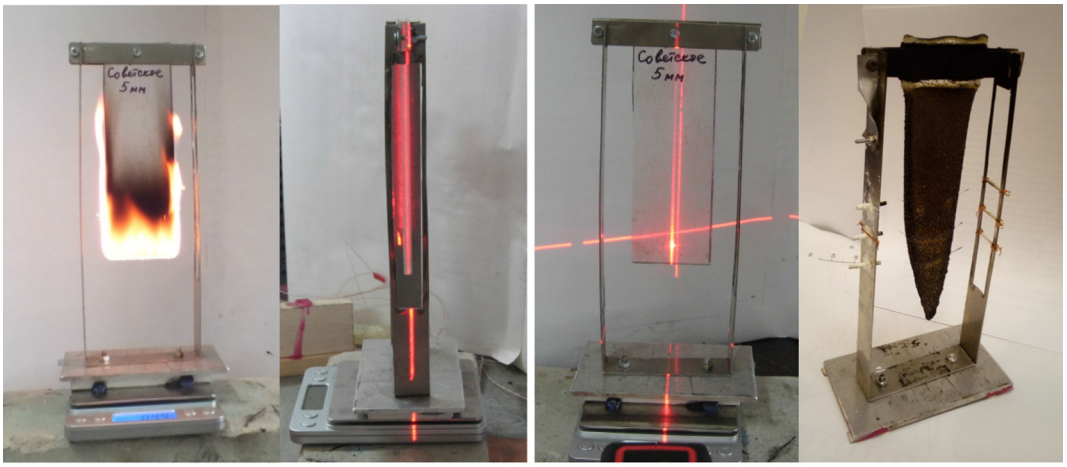

Fig. 2. Upward flame spread experiments (a) burning specimen (front view), (b) laser leveling (side view), (c) laser leveling (front view) and (d) burned specimen.

[20] reported that PMMA begins to soften and melt around 100 °C. At 250 °C, thermal degradation (pyrolysis) of the polymer occurs yielding the monomer, MMA. However, the boiling point of the monomer is 101 °C. Hence, at 250 °C, where pyrolysis occurs, the monomer liquid is hot enough to instantly vaporize and yield monomer vapor. Therefore, at 250 °C, a single-step pyrolysis process (equivalent to sublimation) was assumed as follows:

$$\left[(-C_5H_8O_2-)_n\right]_{solid} \rightarrow n[C_5H_8O_2]_{vapor}$$

In this methodology, FDS incorporates the gasification/sublimation process using an approach utilized for liquid fuel vaporization, where latent heat of vaporization and boiling point are specified. In this case, pyrolysis temperature (250 °C), heat or enthalpy of pyrolysis (Table 1) is specified. Based on this, the mole fraction of the fuel vapor at the fuel surface is calculated.

The mass gasification rate [35] is calculated as,

$$\dot{m}'' = h_m \frac{\bar{p}_m W_F}{RT_g} \ln\left(\frac{X_{F,g}-1}{X_{F,f}-1}\right); h_m = Sh\frac{D_{l,g}}{L},$$

where $\bar{p}_m$ is background pressure, W_F is molecular weight of the fuel, Sh is Sherwood number, T_g is temperature, $X_{F,g}$ is the mole fraction of the fuel vapor in the cell adjacent to the fuel surface and $X_{F,f}$ is the volume fraction of the fuel vapor at the surface, which is a function of surface temperature, given as,

$$X_{F,f} = \exp\left[-\frac{h_v W_F}{R}\left(\frac{1}{T_s}-\frac{1}{T_b}\right)\right],$$

where h_v is heat of pyrolysis, T_s is surface temperature and T_b is PMMA pyrolysis temperature (Table 1). The Sherwood number is computed as,

$$Sh = 0.037Sc^{(1/3)}\mathrm{Re}^{(4/5)},$$

Table 1
Properties of PMMA.

Property	Units	Value	Reference
Density	kg/m^3	1190	[20]
Specific heat	kJ/kg/K	2.1	[20]
Conductivity	W/m/K	0.26	[20]
Emissivity	–	0.85	[35]
Absorption coefficient	m^{-1}	2700	[35]
Pyrolysis temperature	°C	250	[20]
Enthalpy of pyrolysis	kJ/kg	1620	[20]

where Sc is Schmidt number taken as 0.6 and Re is Reynolds number calculated based on the conditions in the cell adjacent to the fuel surface. The net contribution of thermal radiation in the energy equation is given as:

$$\dot{q}_r''' \equiv -\nabla.q_r''(x) = \kappa(x)[U(x) - 4\pi I_b(x)];\ U(x) = \int_{4\pi} I(x,s')ds',$$

where $\kappa(x)$ is the local absorption coefficient, $I_b(x)$ is the source term, and $I(x,s)$ is the solution to the Radiation Transport Equation (RTE) for a non-scattering gray gas, written as,

$$S\cdot\nabla I(x,s) = \kappa(x)[I_b(x) - I(x,s)]$$

The mean absorption coefficient κ, is a function of species composition and temperature. FDS obtains these values from narrow-band model called RadCal [35].

It should be noted that the solid phase mass regresses cell by cell based on the gasification mass flux. The actual regression of the solid phase and the shape of pyrolysis front have not been modeled by FDS. Based on the mass burning rate, the regression rate can be calculated.

In the numerical model of Wang and Chateil [25], the pyrolysis has been modeled using ignition temperature, heat of vaporization and the heat release rate. In the present study, pyrolysis temperature and heat of pyrolysis are specified, which is then used in Stefan's diffusion equation to predict the mass loss rate. This approach is simpler, however, it only models pyrolysis as a sublimation process.

It is clear from the experiments that the processes of upward and downward flame spread over PMMA slabs are symmetric in relation to the thickness of the specimen. Hence the computational domain involves thickness symmetry. Fig. 3 shows the computational domain for two cases; downward spread over a 5.4 mm-thick slab and upward spread over a 5 mm-thick slab. The left side of the boundary is a symmetric boundary. The first-order derivative of all variables (other than X-component velocity) is set to zero, and the X-component velocity is set to zero. The top and right boundaries are open boundaries, where the combustion products may leave or atmospheric air can come into the domain. Here, pressure is atmospheric pressure and variables are extrapolated from interior. For incoming flow, mass fraction of oxygen and nitrogen are set as 0.23 and 0.77, respectively, and temperature is set as ambient temperature. The bottom of the domain is an inert wall, which is specified to be adiabatic for temperature, zero diffusive flux for species and no slip for velocities. Initially in the

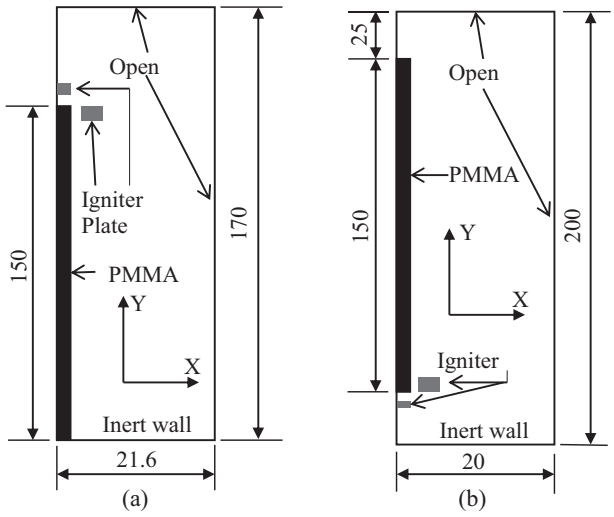

Fig. 3. Computational domain (all units are in mm) for (a) downward spread over 5.4 mm thick PMMA and (b) upward spread over 5 mm thick PMMA.

domain, the mass fraction of oxygen is set as 0.23, (rest nitrogen) the temperature is set as the ambient temperature.

The length and width of the PMMA specimen are 150 mm × 50 mm. Simulations were carried out with coarse grids and based on the results obtained, intermediate and fine grids have been used. It is observed that in order to capture the temperature and species profiles, a cell size of around 0.4 mm–0.5 mm is required in the X-direction. In order to capture the flame spread rate, a cell size of at least 1 mm is required in the Y-direction. A multi-block structured mesh has been used in this study. Since flame anchors through the entire width, either a single cell or utmost 3 cells have been used in that direction to reduce the computational expense. For instance, for downward flame spread in 5.4 mm thick slab, top 60 mm height has been provided with fine mesh, and the bottom portion has been coarsely meshed. For investigating steady flame propagation in this problem, this approach seems to be economical. Heating surfaces, called igniter plates, are used to onset the ignition. They are shown in Fig. 3. They are set to temperature in the range of 1000 °C–1200 °C, so that the specimens heat up. Once the specimen is ignited, as observed by the temperature contours, the hot plates are removed from the domain.

The combustion of monomer vapors with air can be written in term of the global reaction given by:

$$C_5H_8O_2 + 6(O_2 + 3.76N_2) \rightarrow 5CO_2 + 4H_2O + 22.56N_2$$

Since the flame established over the PMMA surface is a diffusion flame, the transport of fuel vapor and air dictates the reaction process. Therefore, the infinite rate chemistry option available in FDS has been employed to combustion of the monomer vapors.

3. Results and discussions

3.1. Validation of FDS results against results from Ananth et al. [20]

Ananth et al. [20] have numerically predicted the temperature profiles for boundary layer combustion over horizontal flat PMMA slab under forced convective conditions. These represent the cases of concurrent flame spread where flame rapidly spreads over the fuel surface due to concurrent forced convection. The length and thickness of the PMMA slab are 67 mm and 25.4 mm, respectively. Since the fuel sample is much thicker, once the flame spreads over the sample, it anchors over the fuel surface as a boundary layer flame and consumes the fuel at an almost steady rate. When compared to upward flame spread over vertically oriented sample under natural convection, this concurrent case is much controllable because of the presence of forced convection. A particular case with an air velocity of 1.69 m/s has been chosen for validation. A computational domain provided in Ananth et al. [20] has been used in the validation studies. After performing a grid independence study with grid sizes of 0.5 mm, 0.25 mm and 0.35 mm, near the PMMA surface, a grid size of 0.35 mm is used to obtain the temperature profiles in the direction perpendicular to the fuel surface.

Ananth et al. [20] have reported both predicted and measured temperature profiles at four locations along the PMMA surface for different air velocities. Fig. 4 shows the predictions by FDS, compared against the experimental and numerical results reported in Ananth et al. [20]. It is clear that there are notable discrepancies in the temperature profiles near the fuel surface. The temperature very near to the surface is over-predicted by FDS. Infinite rate chemistry employed in FDS may be the reason for this. The heat flux to the fuel surface $[(k\partial T/\partial y)_{y=0}]$, has been estimated by calculating the temperature gradient at the surface from the temperature profiles. The thermal conductivity, k, has been estimated as that of air at the surface temperature. The comparison of surface heat flux, estimated by this method, is shown in Fig. 5. It is clear that, the predicted heat flux trend agrees quite well with the experimental data of Ananth et al. [20], even though the temperature predictions near the surface is higher than the experimental data. FDS is able to predict the slope value of temperature profile near the surface reasonably well. It should also be noted that the location of the peak temperature is predicted very well. This shows that the central reaction zone can be predicted reasonably well by FDS. Further, the portion of the profile extending from the peak location towards ambient is also predicted very well by FDS, as predicted by the numerical model of Ananth et al. [20]. Keeping in mind the simplicity of FDS, the results obtained may be considered as quite reasonable.

3.2. Upward flame propagation

Upward flame propagation has been studied using PMMA slabs of 1.6 mm, 2.4 mm and 5 mm thickness. From the time of ignition, the flame grows in length to engulf the whole sample. However, the flame anchoring point remains fixed almost at the bottom of

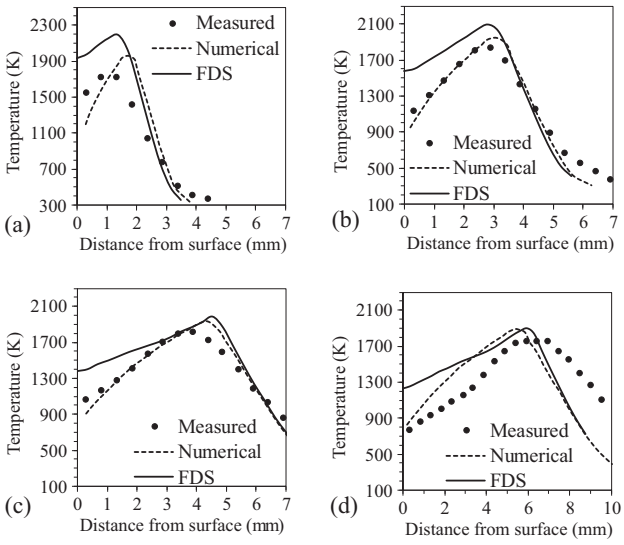

Fig. 4. Validation of FDS results using data from Ananth et al. [20]. Symbols: experimental results [20], dashed lines: numerical results [20] and solid lines: FDS, at X locations of (a) 10, (b) 20, (c) 35 and (d) 55 mm.

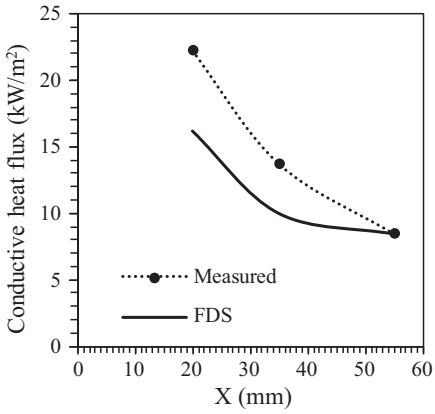

Fig. 5. Comparion of surface heat flux estimated using temperature profiles from the experimental data [20] and present FDS simulations.

the plate and thus, there is no propagation of flame anchor point. The upward burning process is unsteady in nature. Temporal variation in mass loss rates as obtained from FDS simulations have been compared with the measured data in Fig. 6. The mass loss rate was found to increase with time, with oscillations in the temporal data. This is due to increase in the pyrolysis length and surface which induce buoyancy induced flow, with time.

Numerical results are plotted for the time up to which the present experimental data have been recorded. The numerical model in FDS is able to clearly predict the variation trend for all the cases. It should be noted that in the smaller thickness case, the slab warped due to immense heat transfer from the flame and that quartz wire has been used to stiffen the form against warping. However, this phenomenon has not been modeled. The initial over-prediction of the mass loss rate by FDS is due to the presence of an ignition source. In fact, ignition was onset quite carefully by using heating plates of temperature of 1000 °C for the minimum time within which the specimen is ignited. It is tested that if the ignition source is removed before that time, flame would not anchor. For sample of 1.6 mm thickness, ignition source is kept for around 25 s; however, no significant hike in the mass loss rate is observed. In 2.4 mm and 5 mm cases, similar ignition sources are used, but for slightly longer time of around 35 s. However, the mass loss rate is higher for these cases during the ignition period. Further, the mass loss rate was quite high for 5 mm case during this period and formed a major discrepancy between the FDS prediction and experimental data.

Fig. 7 shows the X temperature profiles at Y-locations of 50 mm, 100 mm and 150 mm of the sample, measured from the leading edge, for the upward flame spread over 2.4 mm thick PMMA slab at a time instant of 90 s. The temperature profile starts with the cell centered temperature just next to the solid surface and does not include the surface temperature.

It is apparent from Fig. 7 that for the case of upward flame spread, the peak temperature decreases and its location increases as the Y-location increases. Flame, as it spreads, anchors more close to the sample at the bottom and its stand-off distance increases towards the top portion of the sample. This results in a shift of the maximum temperature location away from the fuel surface. FDS is able to predict these physics correctly.

Fig. 8 presents the grayscale temperature contour superimposed by velocity vectors as predicted by FDS for the upward flame spread over PMMA of different thickness. Coordinates and dimensions are as indicated in Fig. 3. Here, the flame anchors around the same location for all the cases as well as it is spread over the entire length. That is, the flame is tall enough due to buoyancy driven flow and heats up considerable portion of the PMMA sample. Velocity vectors clearly show the entrainment of ambient air. The velocity value becomes the maximum at the flame zone due to the acceleration of hot gases in the high temperature region. Velocity increases in the flame spread direction. When the maximum velocity values at a Y-location of 60 mm is compared, it is found that for 1.6 mm, 2.4 mm and 5 mm thicknesses, maximum velocity values are 1.04 m/s, 0.966 m/s and 0.9 m/s, respectively. At Y = 80 mm, the corresponding values are 1.34 m/s, 1.19 m/s and 1.23 m/s, respectively. Thus, the maximum velocities at a given Y are found to be in the similar order.

3.3. Downward flame propagation

Unlike upward flame propagation, the downward flame spread process is much slower. This facilitates field measurement of major chemical species and temperature, and thus, a detailed flame structure can be determined. Fig. 9 presents the experimentally measured temperature field for downward flame spread in PMMA slabs of 1.6 mm and 5.4 mm thick. The flame anchoring and its

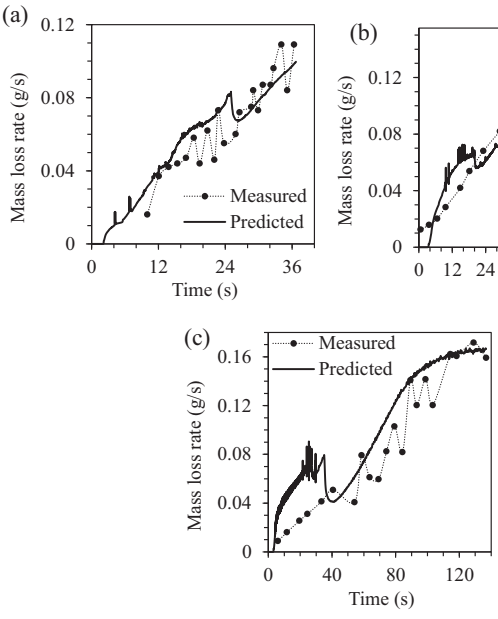

Fig. 6. Comparison of the predicted mass loss rate against the corresponding experimental data for upward flame spread over PMMA slab of thickness of (a) 1.6 mm, (b) 2.4 mm and (c) 5 mm.

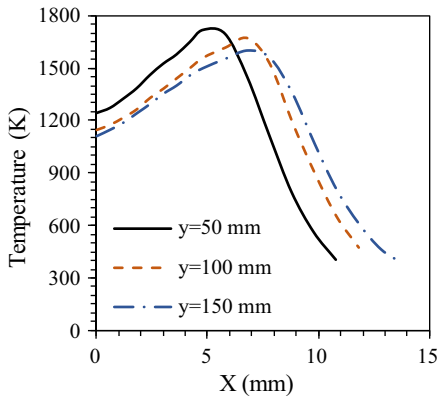

Fig. 7. X temperature profiles at various Y locations for the upward flame spread over 2.4 mm thick PMMA slab at a time instant of 90 s.

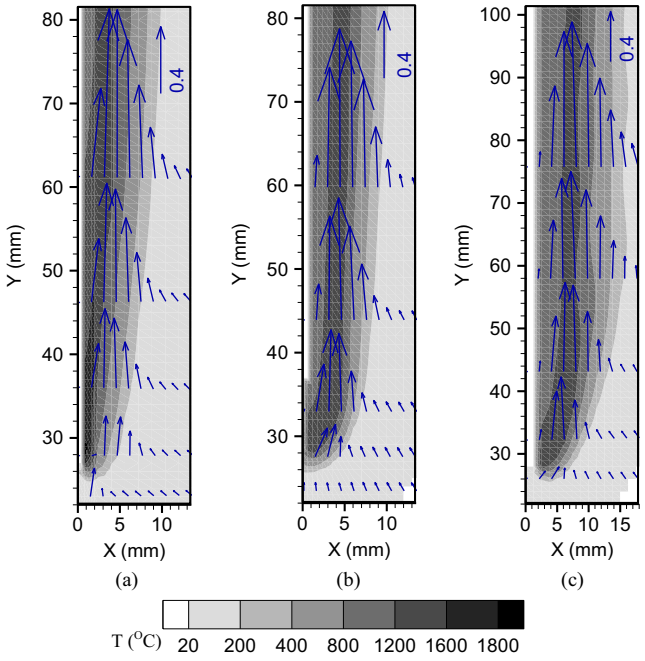

Fig. 8. Temperature contours with velocity field for the upward flame spread over PMMA slab with thickness of (a) 1.6 mm, (b) 2.4 mm and (c) 5 mm.

shape are almost similar between these cases. In the case of 5.4 mm thickness, it is clear that the solid portion where the flame anchors is triangular in shape. It may be noted that in the plots the Y-coordinate is set to zero around the base of the triangle. FDS is not built-in with two-phase model, which can accomplish this pyrolysis physics as observed in experiments.

The predictions of temperature and velocity fields by FDS for these cases are shown in Fig. 10. Coordinates and dimensions in Fig. 10 are as given in Fig. 3. Air entrainment from the ambient, velocity overshoot in the flame zone and buoyancy driven flow are clearly predicted by FDS. Unlike the upward flame propagation, the numerical prediction of downward flame propagation is quite involved, as pointed out by previous researchers [8]. This is because of the fact that the flame propagation is slow and the flame heats up only a little portion of the PMMA ahead of its propagation. Fine meshes in both the flame spread direction, as well as in the direction perpendicular to it, are required in order to capture this phenomenon.

The mass loss rates as predicted by FDS for the two cases are shown in Fig. 11. Mass loss rate becomes nearly steady for the 1.6 mm case after around 80 s. The ignition source for both of these cases has been removed around 35 s. The mass loss rate or the burning rate (in g/s), as predicted by FDS, is recorded every time step. The burning rate is estimated from FDS simulation is 0.012 g/s for 1.6 mm case, which is quite close to the experimentally determined value of 0.0119 g/s. The flame spread velocity is computed using the position of the flame front relative to the leading edge. The corresponding predicted and measured flame spread velocities are 0.126 mm/s and 0.12 mm/s, respectively.

For the 5.4 mm case, the flame spread process is unsteady for much prolonged duration, compared to 1.6 mm case. The mass loss rate is still seen to be approaching the steady state at 200 s. The flame spread rate, pyrolysis length and flame length also exhibit unsteady growth similar to mass loss rate. Thus, notable discrepancies are observed in the predicted burning rate (around 0.03 g/s) against the measured value (around 0.02 g/s) in this study. Similar measured values are reported by Gong et al. [21]. The predicted flame spread velocity is around 0.08 mm/s, as compared to the measured value of 0.065 mm/s. In literature, typical measured flame spread velocity values of 0.075 mm/s and 0.06 mm/s, are reported in Refs. [36] and [37], respectively. Similarly, values of 0.09 mm/s and 0.18 mm/s were reported using computational [15] and theoretical [16] studies.

Predicted and measured temperature profiles in X- and Y-directions are shown in Figs. 12 and 13, respectively, for the case of downward flame spread in the 1.6 mm PMMA slab. It is quite apparent that the X-profiles at several Y-locations, which represent the flame structure, have been predicted quite reasonably by FDS, as it predicted the results of Ananth et al. [24]. In particular, the curves going towards the ambient match the measured data well. Near to PMMA surface, the predictions are quite off, as observed in the validation case. The mismatch between predicted and experimental measurements in temperature, which is the largest near the flame anchoring region (around Y = 2 mm) is probably due to infinitely fast kinetics sub-model used in FDS. This results in higher temperature close to the fuel surface. This suggests that although the flame is diffusion-controlled, kinetics has some effect, and that needs to be modeled. The agreement between prediction and experimental measurement improves at distance further downstream of flame anchoring point. At farther Y-locations (>6 mm),

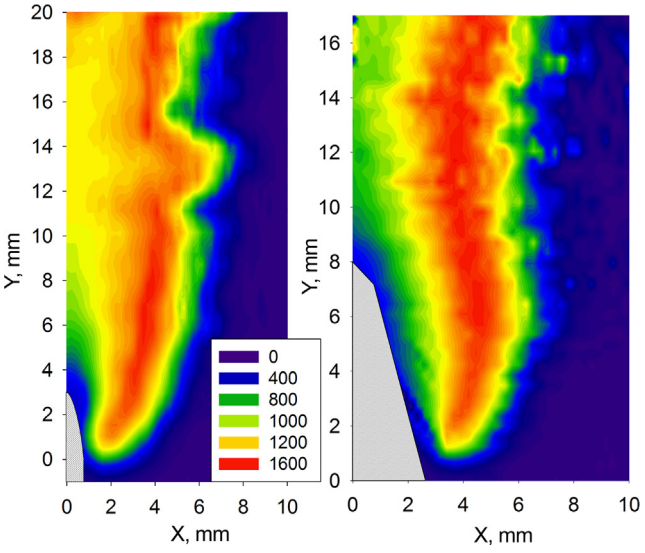

Fig. 9. Temperature contours as measured in experiments for downward flame spread over PMMA slab with thickness of 1.6 mm (left) and 5.4 mm (right).

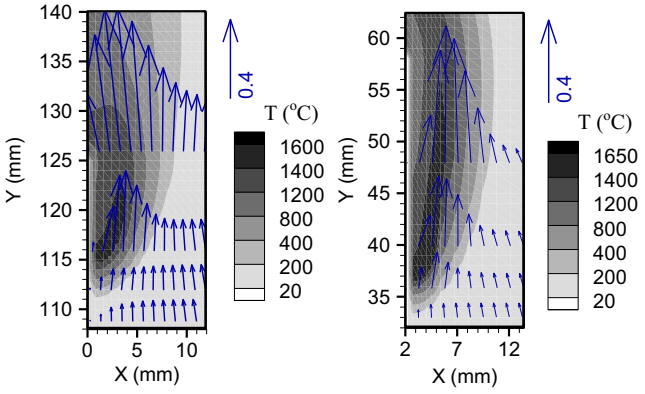

Fig. 10. Gas-phase temperature contours and velocity field predicted by FDS for downward flame spread over PMMA slab with thickness of 1.6 mm (left) and 5.4 mm (right).

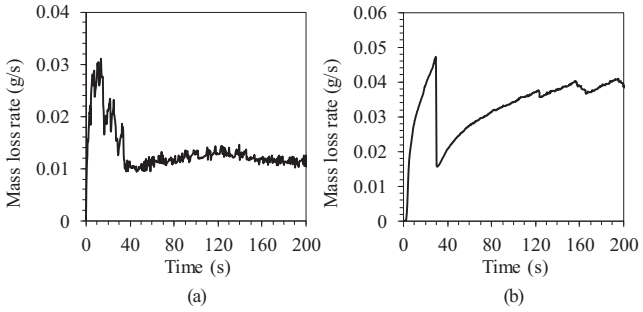

Fig. 11. The predicted mass loss rate for downward flame spread over PMMA slab with thickness of (a) 1.6 mm and (b) 5.4 mm.

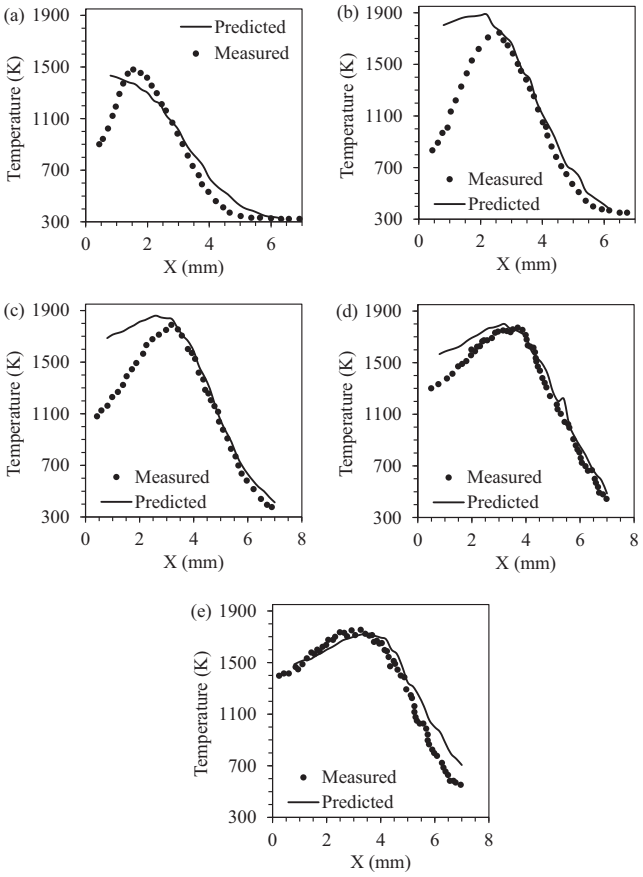

Fig. 12. Predicted and measured temperature profiles along X-direction at Y locations of (a) 2 mm, (b) 4 mm, (c) 5.6 mm, (d) 9.3 mm and (e) 12.8 mm for the downward flame spread over 1.6 mm thick PMMA fuel, where Y = 0 mm location corresponds to the beginning of the pyrolysis zone.

the peak and the location of the peak in the predicted profiles match the measured data well. Similarly, the Y-profiles of temperatures predicted by FDS at two X-locations match the measured data quite well, as shown in Fig. 13. It is apparent that the Y-direction gradient at both X-locations has been captured by the numerical model sufficiently well. Further, the peak location and the decreasing trend after the attainment of the peak value are also predicted reasonably well. Fig. 13(a) also shows that near the surface of PMMA, the difference between measured and predicted temperatures is maximum (near Y = 0) due to the reason mentioned above. However, the agreement is quite good away from Y = 0.

The predicted X-profiles of mole fractions of oxygen, CO_2 and H_2O for 1.6 mm downward flame spread have been shown in

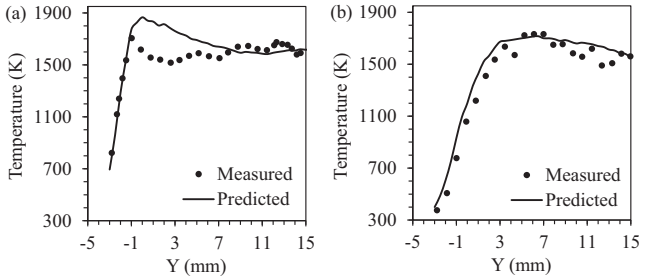

Fig. 13. Predicted and measured temperature profiles along Y-direction at X locations of (a) 2 mm and (b) 4 mm for downward flame spread over 1.6 mm thick PMMA fuel, where X = 0 mm location corresponds to the centerline of the specimen.

Fig. 14. These are plotted at a given time instant where the temperature profiles have been plotted. In fact, after around 80 s, the downward flame spread over 1.6 mm thick PMMA slab has been almost steady. Thus, any time instant after 80 s, would provide similar profiles. As the height from the pyrolysis zone (Y) increases, oxygen penetration towards the PMMA specimen is observed. Its mole fraction at a given X-location decreases as Y is increased. The gradient of oxygen mole fraction increases with increase in Y-location indicating its faster consumption at those locations. On the other hand, the mole fractions of CO_2 and H_2O increase as Y is increased. These products formed at the high temperature zone are transported away towards the ambient. The gradient of the mole fractions of these two species increases with increase in Y-location, showing the sharp gradients of species around the flame zone.

Fig. 15 shows the grayscale mole fraction contours of O_2, CO_2 and H_2O for the case of downward flame spread over a 1.6 mm-thick PMMA slab, at the same time instant when the profile data are extracted. Coordinates and dimensions in Fig. 15 are as indicated in Fig. 3. In these contours, the Y-location has been marked as per the dimensions of the computational domain. It is clear that as oxygen is consumed in the flame zone, products such as CO_2 and H_2O are formed and transported to the inner (fuel and flame) and

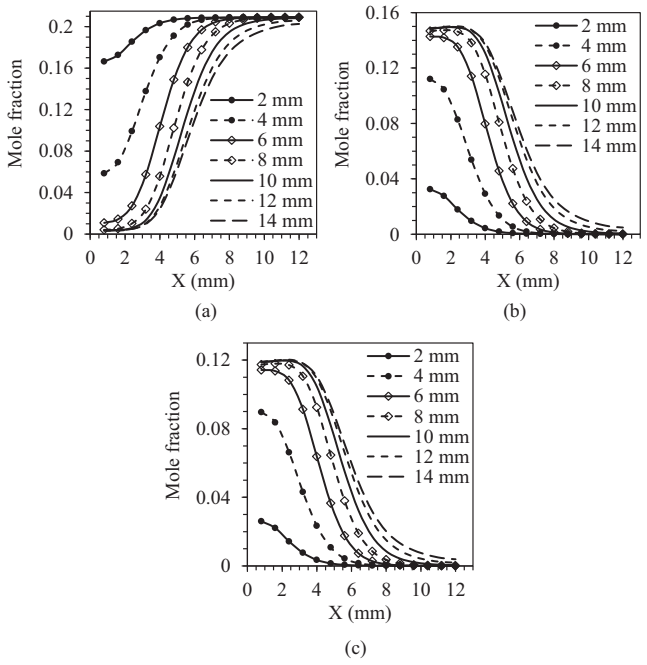

Fig. 14. Predicted X-profiles of mole fraction of (a) oxygen, (b) CO_2 and (c) H_2O for downward flame spread over 1.6 mm thick PMMA slab.

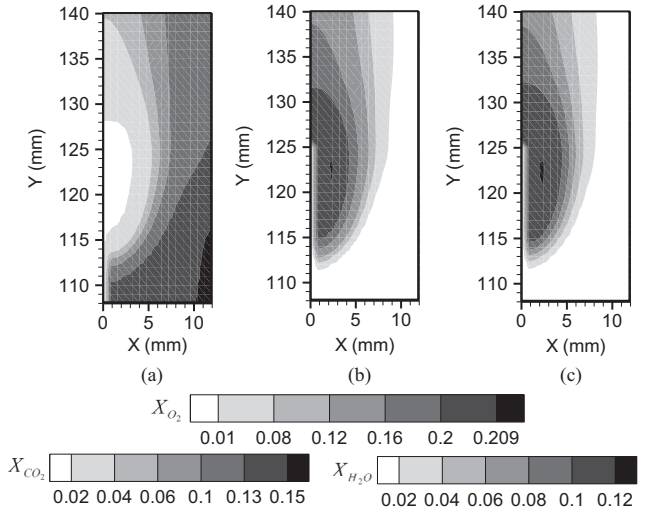

Fig. 15. Predicted contours of the mole fraction of (a) oxygen, (b) carbon dioxide and (c) water vapor for downward spread over a 1.6 mm thick PMMA slab.

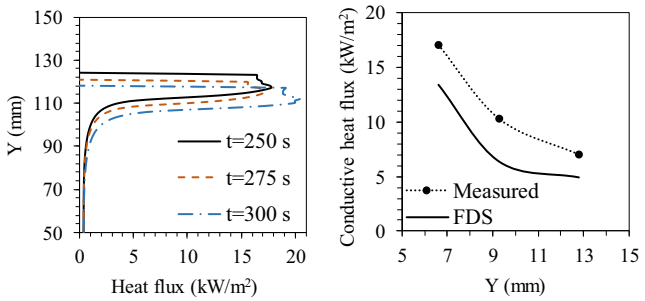

Fig. 16. Variation of predicted heat flux along the surface (left) and the heat flux at various Y locations as calculated by the X temperature profiles (right), for downward flame spread over 1.6 mm thick PMMA slab.

outer (ambient and flame) zones. Oxygen penetration is the key aspect for the mass burning rate in the case of flame established over condensed fuel surfaces.

From Figs. 12–15, it is clear that FDS is able to predict the temperature and species fields reasonably well for the steady flame propagation over a PMMA slab, especially in the gas-phase, when simulations have been carried out with simplified sublimation type boundary condition at the interface.

Average value of total incident heat flux on the surface of the PMMA is obtained from FDS and the variation of heat flux along the surface is shown in Fig. 16 (left). As mentioned in the FDS manual [35], the total incident heat flux is the incoming radiative heat flux. In Fig. 16, for each time instant, the location at which the heat flux drops to a zero value indicates that there is no material present above that. This can be used to assess the regression rate or the flame spread rate. For instance, at 250 s, the zero heat flux location is at around 123 mm, for 275 s, it is at around 120 mm and for 300 s, it is at around 117 mm. Using the distance regressed and the time elapsed, the regression rate, from the heat flux can be estimated as 0.12 mm/s. This value is quite close to that obtained using the burning rate. This shows that the mass loss rate and flame spread rate are proportional to the heat flux to the surface. The heat flux to the fuel surface $[(k\partial T/\partial x)_{x=0}]$, has been estimated by calculating the temperature gradient at the surface from the X temperature profiles. A comparison between experimental and FDS results is shown in Fig. 16 (right). As seen in the validation case, the trend is preserved in the predicted results, even though the values are consistently under-predicted.

For 5.4 mm thickness case, which has been observed to be quite unsteady from the mass loss rate data in Fig. 11(b), the experimentally measured O_2, CO_2 and H_2O contours are shown in Fig. 17. The PMMA slab is shown as a shaded area. It is apparent that the reaction zone is thicker and increased penetration of the products towards the PMMA surface is observed.

Fig. 18 presents the contours of the mole fractions predicted by the numerical model for the same case shown in Fig. 17, close to the top portion of PMMA. Coordinates and dimensions in Fig. 18 are as shown in Fig. 3. Numerical results also show a thicker reaction zone and increased penetration of the products towards the PMMA. Even though waviness is observed in the experimental contours, numerical contours do not show such a phenomenon.

For a heterogeneous diffusion flame, oxygen transport is extremely important. Fig. 19 presents the X-profiles of oxygen mass fraction at several Y-locations for the case of downward flame spread over 5.4 mm PMMA slab, as predicted by the numerical model, compared with the experimental measurements.

It is observed that oxygen transport has been predicted reasonably well through the height of the PMMA slab. The major discrepancy is seen at Y = 0, close to fuel surface, where almost complete consumption of oxygen is predicted, as against the experimental results, which show significance presence of oxygen. This suggests the need of short chemical kinetics mechanism to predict these more accurately.

It is clear that, as Y increases, oxygen penetration towards the PMMA slab increases and it is also consumed as it is transported. The oxygen mole fraction asymptotically varies from its ambient value, decreases sharply and asymptotically gets consumed in the flame zone. The location where it is consumed increases with Y, reaches a maximum and decreases to remain a constant.

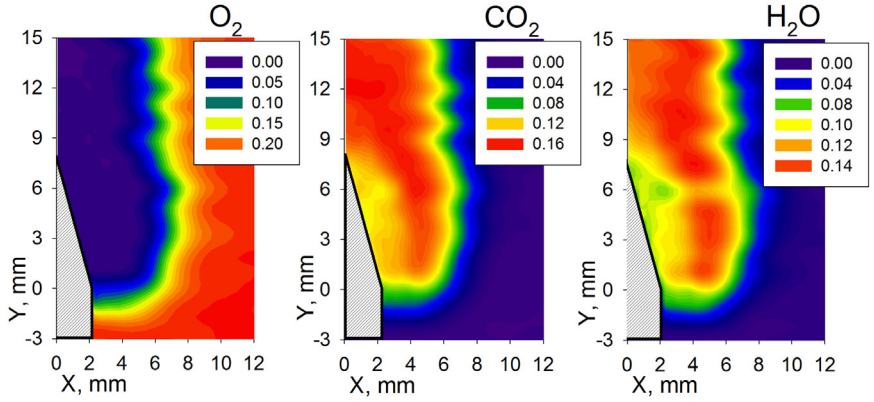

Fig. 17. Experimentally measured contour plots for oxygen, carbon dioxide and water vapor for the case of downward flame spread over PMMA slab 5.4 mm thick.

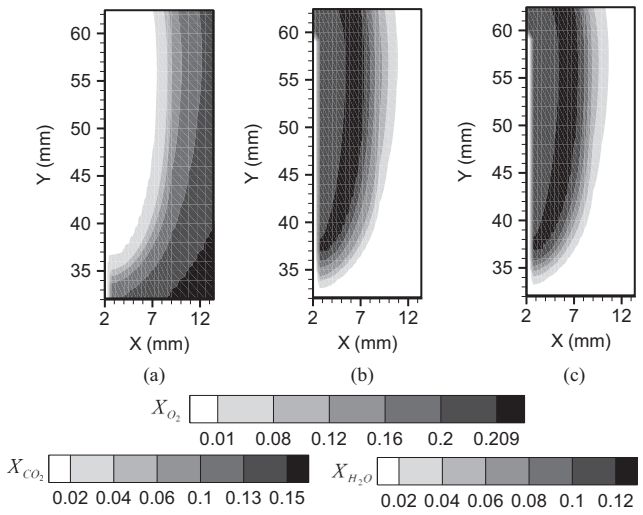

Fig. 18. Predicted contour plots of (a) oxygen, (b) carbon dioxide and (c) water vapor mole fractions for the downward flame spread over 5.4 mm thick PMMA slab for the numerical results.

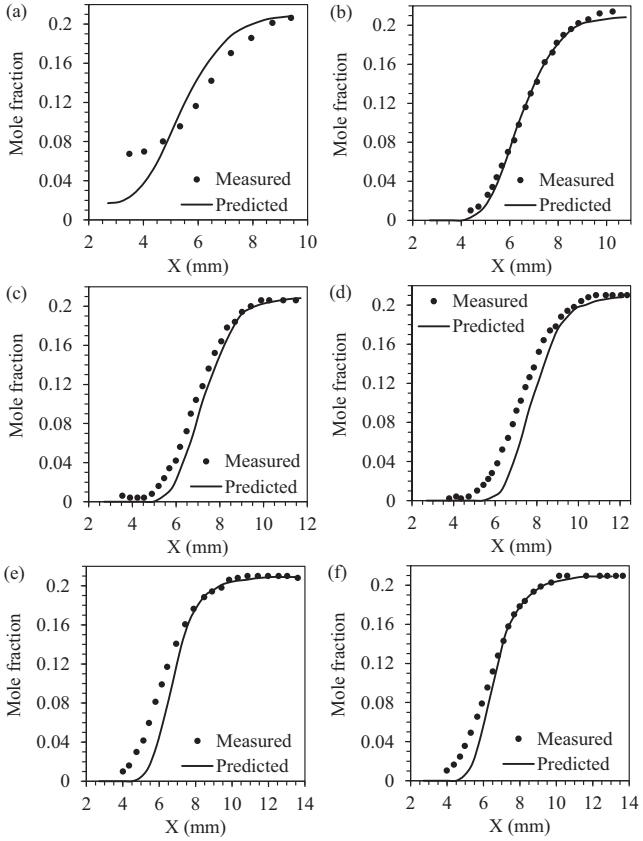

Fig. 19. X-profiles of the oxygen mole fraction at Y locations of (a) 0 mm, (b) 2 mm, (c) 4 mm, (d) 6 mm, (e) 8 mm and (f) 10 mm for downward spread flame over a 5.4 mm thick PMMA slab.

4. Summary and conclusions

Experimental and numerical investigations of upward and downward flame spread over PMMA slabs of various thickness have been carried out. Downward flame spread has been analyzed using PMMA slabs 1.6 mm and 5.4 mm thick, while the upward spread has been analyzed using slabs 1.6 mm, 2.4 mm and 5 mm thick.

Detailed measurements of burning/regression rate, species and temperature field have been carried out on during the study of burning of non-charring PMMA. A simple and computationally economical numerical model, FDS, has been used to simulate the experimental cases. Pyrolysis or gasification of PMMA has been modeled similar to a sublimation process. Infinite rate chemistry has been used to model chemical reaction. Study of species profiles such as oxygen will help in better understanding of the nature of consumption of the oxidizer thereby indicating the important role played by air entrainment in assisting the spread of fire over a surface.

For upward flame propagation, the mass loss rates or burning rates have been predicted by the numerical model. The upward burning process over finite length PMMA slab is inherently unsteady. The burning rate increases with time during upward flame propagation due to the existence of taller buoyancy driven flame and the heat transfer from it to the downstream PMMA surface. The temporal variation of the mass loss rate compares reasonably well with that of the measured values, especially for lower thickness cases. During ignition, the mass loss rate has been over-predicted for thicker PMMA slabs. Temperature and velocity fields have been predicted by the numerical model to understand the flame stand-off and the velocity overshoot.

The downward flame propagation is usually known to quickly attain steady state after ignition for thin fuels. However, for thick fuels, the flame spread process exhibits an unsteady behavior. A steady state spread rate was attained at about 80 s in the 1.6 mm case. The case with 5.4 mm thickness was seen to still approach steady state even at 200 s. Thus, for thicker fuels, the steady spread may be attained after several minutes. During this period, the flame spread rate and flame length and pyrolysis length also increase unsteadily approaching a steady state value. The downward spreading flame over thicker fuel tends to be longer than that over a thinner fuel.

The numerical model has been able to predict the burning rate and the flame spread rate for the case of 1.6 mm thick PMMA slab, much close to the experimentally determined values. There has been discrepancy in the prediction of the burning rate for the case of 5.4 mm. The numerical model has predicted the temperature profiles for the case of 1.6 mm closer to the experimentally measured values. In terms of temperature and species profiles, the flame structure has been presented in detail. For the 5.4 mm case, X-profiles of oxygen have been predicted closer to the experimentally measured values. It is interesting to note that even though FDS uses infinite kinetics model for chemistry, the global trends are predicted reasonably well. This could be explained to be due dependence of global trends like flame spread rate, mass loss rate, flame length etc. on integral of quantities like heat flux from the flame to the fuel surface which in turn are dependent of heat and mass transport process in diffusion flame. The observed discrepancy especially in local prediction of species and temperature (and some consequence on integral quantities) were found to occur at flame anchor region due to assumption if infinite kinetics.

Overall, reliable experimental data and numerical results from an economical computational model have been presented. This data may be quite useful in understanding the structure and spread characteristics of flame spread over PMMA slabs and in validating new numerical models.

Acknowledgement

The authors acknowledge funding from Joint RFBR/DST Grant 16-49-02017.

Appendix A

1. FDS input file for downward flame spread over 5.4 mm thick PMMA slab

```
&HEAD CHID='Pmma_5pt4', TITLE='Pmma_5pt4_Downward'  /

&MESH IJK=12,1,80, XB=0.0,0.0054,0.0,0.005,0.09,0.170 /
&MESH IJK=10,1,80, XB=0.0054,0.0189,0.0,0.005,0.09,0.170 /
&MESH IJK=14,1,90, XB=0.0,0.0189,0.0,0.005,0.0,0.090 /

&MISC RESTART=.FALSE. /
&TIME T_END=350. /

&SPEC ID ='PMMA',FORMULA='C5.0H8.0O2.0'/
&SPEC ID ='OXYGEN',MASS_FRACTION_0=0.232/
&SPEC ID ='CARBON DIOXIDE'/
&SPEC ID ='WATER VAPOR'/
&SPEC ID ='NITROGEN',MASS_FRACTION_0=0.768/

&REAC ID = 'pmma'
          FUEL='PMMA'
          HEAT_OF_COMBUSTION=25200.
          SPEC_ID_NU='PMMA','OXYGEN','CARBON DIOXIDE','WATER VAPOR'
           NU=-1,-6,5,4/

&SURF ID           = 'PMMA_solid'
      COLOR        = 'IVORY BLACK'
      MATL_ID      = 'PMMA_mat'
      BURN_AWAY    = .TRUE.
      THICKNESS    = 0.0027 /

&MATL ID           = 'PMMA_mat'
      EMISSIVITY   = .85
     DENSITY       = 1190
     CONDUCTIVITY  = 0.26
     SPECIFIC_HEAT = 2.1
        NU_SPEC     = 1.
        N_REACTIONS = 1
        SPEC_ID     = 'PMMA'
       BOILING_TEMPERATURE=250.
        HEAT_OF_REACTION= 1620 /

&OBST XB=0.00,0.0027,0.0,0.005,0.00,0.15, SURF_ID='PMMA_solid'/

&OBST XB = 0.005,0.008,0.0,0.005,0.145,0.15,
SURF_ID='IGNITER',DEVC_ID='Timer1' /
&SURF ID='IGNITER', TMP_FRONT=1000,COLOR='GREEN' /
&DEVC XYZ=0.006,0.003,0.146,ID='Timer1',
QUANTITY='TIME',SETPOINT=35.0, INITIAL_STATE=.TRUE. /
```

```
&OBST XB = 0.0,0.0027,0.0,0.005,0.153,0.156,
SURF_ID='IGNITER1',DEVC_ID='Timer2' /
&SURF ID='IGNITER1', TMP_FRONT=1000,COLOR='GREEN' /
&DEVC XYZ=0.002,0.003,0.154,ID='Timer2',
QUANTITY='TIME',SETPOINT=35.0, INITIAL_STATE=.TRUE. /
&VENT MB='XMIN', SURF_ID = 'MIRROR' /
&VENT MB='XMAX', SURF_ID = 'OPEN' /
&VENT MB='ZMAX', SURF_ID = 'OPEN' /

&BNDF QUANTITY='WALL TEMPERATURE' /
&BNDF QUANTITY='INCIDENT HEAT FLUX' /
&BNDF QUANTITY='BURNING RATE' /

&SLCF PBY=.0, QUANTITY='MASS FRACTION',SPEC_ID='PMMA',VECTOR=.TRUE./
&SLCF PBY=.0, QUANTITY='MASS FRACTION', SPEC_ID='OXYGEN',
VECTOR=.TRUE. /
&SLCF PBY=.0, QUANTITY='MASS FRACTION',SPEC_ID='CARBON
DIOXIDE',VECTOR=.TRUE. /
&SLCF PBY=.0, QUANTITY='MASS
FRACTION',SPEC_ID='OXYGEN',VECTOR=.TRUE. /
&SLCF PBY=.0, QUANTITY='MASS FRACTION',SPEC_ID='WATER
VAPOR',VECTOR=.TRUE. /
&SLCF PBY=.0, QUANTITY='MASS
FRACTION',SPEC_ID='NITROGEN',VECTOR=.TRUE. /
&SLCF PBY=.0, QUANTITY='TEMPERATURE',VECTOR=.TRUE. /
&SLCF PBY=.0, QUANTITY='VELOCITY',VECTOR=.TRUE. /

&DUMP DT_RESTART=1.0 /
&TAIL /
```

2. FDS input file for upward flame spread over 2.4 mm thick PMMA slab

```
&HEAD CHID='Pmma_2pt4', TITLE='Pmma_2pt4_Uward'/

&MESH IJK=10,1,200,XB=0,0.006,0,0.005,0,0.200 /
&MESH IJK=10,1,200,XB=0.006,0.016,0,0.005,0,0.200 /

&MISC RESTART=.FALSE./
&TIME T_END = 200.0 /

&SPEC ID ='PMMA FUEL',FORMULA='C5.0H8.0O2.0'/
&SPEC ID ='OXYGEN',MASS_FRACTION_0=0.232/
&SPEC ID ='NITROGEN',MASS_FRACTION_0=0.768/
&SPEC ID ='CARBON DIOXIDE'/
&SPEC ID ='WATER VAPOR'/

&REAC FUEL='PMMA FUEL'
      HEAT_OF_COMBUSTION=25200.
      SPEC_ID_NU='PMMA FUEL','OXYGEN','CARBON DIOXIDE','WATER VAPOR'
      NU=-1,-6,5,4/
&MATL ID              ='PMMA'
      CONDUCTIVITY    = 0.26
      SPECIFIC_HEAT   = 2.1
      DENSITY         = 1190.0
```

```
      EMISSIVITY       = 0.85
      N_REACTIONS      = 1.0
      SPEC_ID          = 'PMMA FUEL'
      NU_SPEC          = 1.0
      BOILING_TEMPERATURE = 250.
      HEAT_OF_REACTION = 1620./

&SURF ID        = 'VERTICAL_PMMA'
      COLOR     = 'INDIAN RED'
      BURN_AWAY = .TRUE.
      MATL_ID   = 'PMMA'
      THICKNESS = 0.0012 /

&OBST XB=0,0.0012,0,0.005,0.025,0.175, SURF_ID='VERTICAL_PMMA' /

&OBST XB = 0.0,0.0012,0.0,0.005,0.020,0.022,
SURF_ID='IGNITER',DEVC_ID='Timer1' /
&SURF ID='IGNITER', TMP_FRONT=1200,COLOR='GREEN' /
&DEVC XYZ=0.001,0.003,0.021,ID='Timer1',
QUANTITY='TIME',SETPOINT=35, INITIAL_STATE=.TRUE. /

&OBST XB = 0.0045,0.007,0.0,0.005,0.025,0.030,
SURF_ID='IGNITER',DEVC_ID='Timer1' /
&SURF ID='IGNITER', TMP_FRONT=1200,COLOR='GREEN' /
&DEVC XYZ=0.005,0.003,0.027,ID='Timer1',
QUANTITY='TIME',SETPOINT=35, INITIAL_STATE=.TRUE. /

&VENT MB='XMIN',SURF_ID='MIRROR'/
&VENT MB='XMAX',SURF_ID='OPEN'/
&VENT MB='ZMAX',SURF_ID='OPEN'/

&SLCF PBY=.0, QUANTITY='MASS FRACTION',SPEC_ID='PMMA
FUEL',VECTOR=.TRUE. /
&SLCF PBY=.0, QUANTITY='MASS
FRACTION',SPEC_ID='OXYGEN',VECTOR=.TRUE./
&SLCF PBY=.0, QUANTITY='MASS FRACTION',SPEC_ID='CARBON
DIOXIDE',VECTOR=.TRUE. /
&SLCF PBY=.0, QUANTITY='MASS
FRACTION',SPEC_ID='OXYGEN',VECTOR=.TRUE./
&SLCF PBY=.0, QUANTITY='MASS FRACTION',SPEC_ID='WATER
VAPOR',VECTOR=.TRUE. /
&SLCF PBY=.0, QUANTITY='MASS
FRACTION',SPEC_ID='NITROGEN',VECTOR=.TRUE. /
&SLCF PBY=.0, QUANTITY='TEMPERATURE',VECTOR=.TRUE. /
&SLCF PBY=.0, QUANTITY='VELOCITY',VECTOR=.TRUE. /

&BNDF QUANTITY='INCIDENT HEAT FLUX' /
&BNDF QUANTITY='RADIATIVE HEAT FLUX' /
&BNDF QUANTITY='WALL TEMPERATURE' /
&BNDF QUANTITY='BURNING RATE' /

&DUMP DT_RESTART=1.0 /
&TAIL /
```

Appendix B. Supplementary material

Supplementary data associated with this article can be found, in the online version, at https://doi.org/10.1016/j.applthermaleng.2017.11.041.

References

[1] J. Gong, Y. Chen, J. Jiang, L. Yang, J. Li, A numerical study of thermal degradation of polymers: Surface and in-depth absorption, Appl. Therm. Eng. 106 (2016) 1366–1379.

[2] M. Newborough, D. Highgate, J. Matcham, Thermal depolymerisation of polymethyl-methacrylate using mechanically fluidised beds, Appl. Therm. Eng. 23 (2003) 721–731.

[3] T. Kashiwagi, Polymer combustion and flammability, Twenty-Fifth Symposium (international) on combustion, Combust. Inst. 25 (1994) 1423–1437.

[4] A. Tewarson, S.D. Ogden, Fire behavior of Poly Methyl Methacrylate, Combust. Flame 89 (1992) 237–259.

[5] F.A. Williams, Mechanisms of fire spread, Symp. (Int.) Combust. 16 (1) (1977) 1281–1294.

[6] A. Fernandez-Pello, T. Hirano, Controlling mechanisms of flame spread, Fire Sci. Tech. 1 (1982) 17–54.

[7] R. Tu, Y. Zeng, J. Fang, Y. Zhang, The influence of low air pressure on horizontal flame spread over flexible polyurethane foam and correlative smoke productions, Appl. Therm. Eng. 94 (2016) 133–140.

[8] A. Fernandez-Pello, F.A. Williams, Experimental techniques in the study of laminar flame spread over solid combustibles, Combust. Sci. Technol. 14 (1976) 155–167.

[9] M. Sibulkin, C.K. Lee, Flame propagation measurements and energy feedback analysis for burning cylinders, Combust. Sci. Tech. 9 (1974) 137–147.

[10] M. Sibulkin, J. Kim, J.V. Creeden jr., The dependence of flame propagation on surface heat transfer I. Downward burning, Combust. Sci. Tech. 14 (1976) 43–56.

[11] A. Fernandez-Pello, R.J. Santoro, On the dominant mode of heat transfer in downward flame spread, seventeenth symposium (International) on combustion, Combust. Instit. 17 (1) (1978) 1201–1209.

[12] A. Ito, T. Kashiwagi, Temperature measurements in PMMA during downward flame spread in air using holographic interferometry, Twenty-first Symposium (International) on Combustion, Combust. Instit. 21 (1) (1986) 65–74.

[13] A. Ito, T. Kashiwagi, Characterization of flame spread over PMMA using holographic interferometry sample orientation effects, Combust. Flame 71 (1988) 189–204.

[14] S. Bhattacharjee, M.D. King, S. Takahashi, T. Nagumo, K. Wakai, Downward flame spread over poly methyl methacrylate, Proc. Combust. Inst. 28 (2000) 2891–2897.

[15] S. Bhattacharjee, M.D. King, C. Paolini, Structure of downward spreading flames: a comparison of numerical simulation, experimental results and a simplified parabolic theory, Combust. Theor. Model. 8 (1) (2004) 23–39.

[16] S. Bhattacharjee, C. Paolini, W. Tran, J.R. Villaraza, S. Takahashi, Temperature and CO_2 fields of a downward spreading flame over thin cellulose: a comparison of experimental and computational results, Proc. Combust. Inst. 35 (2015) 2665–2672.
[17] K.K. Wu, W.F. Fan, C.H. Chen, T.M. Liou, I.J. Pan, Downward flame spread over a thick PMMA slab in an opposed flow environment: experiment and modeling, Combust. Flame 132 (2003) 697–707.
[18] M.B. Ayani, J.A. Esfahani, R. Mehrabian, Downward flame spread over PMMA sheets in quiescent air: experimental and theoretical studies, Fire Saf. J. 41 (2006) 164–169.
[19] Y. Zhang, X. Chen, Y. Song, X. Huang, Y. Niu, J. Sun, The deceleration mechanism and the critical extinction angle of downward flame spread over inclined cellulosic solids, Appl. Therm. Eng. 124 (2017) 185–190.
[20] R. Ananth, C.C. Ndubizu, P.A. Tatem, Burning rate distributions boundary layer flow combustion of a PMMA plate in forced flow, Combust. Flame 135 (2003) 35–55.
[21] J. Gong, X. Zhou, Z. Deng, L. Yang, Influences of low atmospheric pressure on downward flame spread over thick PMMA slabs at different altitudes, Int. J. Heat Mass Transf. 61 (2013) 191–200.
[22] J. Gong, X. Zhou, J. Li, L. Yang, Effect of finite dimension on downward flame spread over PMMA slabs: experimental and theoretical study, Int. J. Heat Mass Transf. 91 (2015) 225–234.
[23] J.L. Consalvi, Y. Pizzo, B. Portiere, Numerical analysis of the heating process in upward flame spread over thick PMMA slabs, Fire Saf. J. 43 (2008) 351–356.
[24] A.S. Rangwala, S.G. Buckley, J.L. Torero, Upward flame spread on a vertically oriented fuel surface: The effect of finite width, Proc. Combust. Inst. 31 (2007) 2607–2615.
[25] H.Y. Wang, B. Chateil, Numerical simulation of wind-aided flame spread over horizontal surface of a condensed fuel in a confined channel, Internat. J. Eng.-Based Fire Code. 9 (2) (2007) 65–77.
[26] A. Kumar, J.S. T'ien, A computational study of low oxygen flammability limit for thick solid slabs, Combust. Flame 146 (2006) 366–378.
[27] S. Sarma, A. Chakraborty, N.M. Manu, T.M. Muruganandam, V. Raghavan, S.R. Chakravarthy, Spatio-temporal structure of vertically spreading flame over non-planar PMMA surfaces, Proc. Combust. Inst. 000 (2016) 1–9.
[28] W. An, R. Pan, Q. Meng, H. Zhu, Experimental study on downward flame spread characteristics under the influence of parallel curtain wall, Appl. Therm. Eng. 128 (2018) 297–305.
[29] W. An, J. Sun, K.M. Liew, G. Zhu, Effects of building concave structure on flame spread over extruded polystyrene thermal insulation material, Appl. Therm. Eng. 121 (2017) 802–809.
[30] K.M. Liang, T. Ma, J.G. Quintiere, and D. Rouson. Application of CFD Modeling to Room Fire Growth on Walls. NIST GCR 03-849, National Institute of Standards and Technology, Gaithersburg, Maryland, April 2003.
[31] S. Hostikka and K.B. McGrattan. Large Eddy Simulations of Wood Combustion. In Proceedings of the Ninth International Interflam Conference, 755–762, Interscience Communications, London, 2001.
[32] J.W. Kwon, N.A. Dembsey, C.W. Lautenberger, Evaluation of FDS V. 4: upward flame spread, Fire Technol. 43 (2007) 255–284.
[33] W.E. Kaskan, The dependence of flame temperature on mass burning velocity, Symp. (Int.) Combust. 6 (1957) 134–143.
[34] O.P. Korobeinichev, L.V. Kuibida, A.A. Paletsky, A.G. Shmakov, Development and application of molecular beam mass-spectrometry to the study of ADN combustion chemistry, J. Prop. Power 14 (6) (1998) 991–1000.
[35] K. McGrattan, S. Hostikka, R. McDermott, J. Floyd, C. Weinschenk, and K. Overholt. Fire Dynamics Simulator, Technical Reference Guide, Volume 1: Mathematical Model. National Institute of Standards and Technology, Gaithersburg, Maryland, USA, and VTT Technical Research Centre of Finland, Espoo, Finland, sixth edition, September 2013. {http://ws680.nist.gov/publication/get_pdf.cfm?pub_id=913619}.
[36] A. Fernandez-Pello, F.A. Williams, Laminar flame spread over PMMA surfaces, Proc. Combust. Inst. 15 (1975) 217–231.
[37] M. Bundy, Flame tracker: development and testing of a new experimental device for investigating downward spreading flames, San Diego State University, USA, 1995, MS Thesis.